



**HAL**  
open science

# Characterisation of the mesoscopic and macroscopic friction behaviours of glass plain weave reinforcement

Lucila Araceli Montero, Samir Allaoui, Gilles Hivet

► **To cite this version:**

Lucila Araceli Montero, Samir Allaoui, Gilles Hivet. Characterisation of the mesoscopic and macroscopic friction behaviours of glass plain weave reinforcement. *Composites Part A: Applied Science and Manufacturing*, 2017, 95, pp.257 - 266. 10.1016/j.compositesa.2017.01.022 . hal-01763182

**HAL Id: hal-01763182**

**<https://hal.science/hal-01763182>**

Submitted on 10 Apr 2018

**HAL** is a multi-disciplinary open access archive for the deposit and dissemination of scientific research documents, whether they are published or not. The documents may come from teaching and research institutions in France or abroad, or from public or private research centers.

L'archive ouverte pluridisciplinaire **HAL**, est destinée au dépôt et à la diffusion de documents scientifiques de niveau recherche, publiés ou non, émanant des établissements d'enseignement et de recherche français ou étrangers, des laboratoires publics ou privés.

# Characterisation of the mesoscopic and macroscopic friction behaviours of glass plain weave reinforcement

L. MONTERO, S. ALLAOUÏ\*, G. HIVET

Univ. Orléans, PRISME, EA 4229, F45072, Orléans, France.

\* Corresponding author ([samir.allaoui@univ-orleans.fr](mailto:samir.allaoui@univ-orleans.fr))

Keywords : A. Fabrics/textiles; A. Yarn; B. Mechanical properties; E. Preforming;

## Abstract

Friction at different levels of the multi-scale structure of textile reinforcements is one of the most significant phenomena in the forming of dry fabric composites. This paper investigates the effect of the test conditions on fabric/fabric and yarn/yarn friction. Friction tests were performed on a glass plain weave and its constitutive yarns, varying the pressure and velocity. The results showed that the friction behaviours at the two scales were highly sensitive to these two parameters. An increase in pressure led to a decrease in the friction coefficients until steady values were reached, while an increase in velocity led to an increase in the friction coefficients. At each scale, the frictional behaviour of the material was significantly influenced by the structural reorganisation of the lower scale.

## 1. Introduction

Fibre-reinforced composite materials are gaining in popularity in industry because of their high performances, lightweight and design flexibility. In addition, textile composites offer sustainable solutions concerning environmental issues, for instance in transport sectors where decreasing the weight of the different structures can reduce fuel consumption and hence polluting emissions. However, even if fibrous composites appear to be a good solution, many issues remain, especially as regards mastering processes such as the predictability of the quality of the part, cycle time, cost price, etc.

Liquid Composite Moulding (LCM) processes are among the most attractive candidates to manufacture complex composite shapes with a high degree of efficiency (cost/time/quality). The first step in LCM processes consists in forming the fibrous reinforcement. The mechanical behaviour of dry reinforcement with respect to the shape geometry is a key point in order to ensure both a correct final shape and good mechanical properties of the final part. In addition, during a multi-layer forming process, friction between the reinforcement layers and between

tools and external layers has a significant effect on the quality of the preform obtained (appearance of defects) [1, 2]. However, the mechanisms governing the preforming of dry reinforcements are far from being fully understood [3]. During preforming, the reinforcements are subjected to different loadings such as tension, shear, compression, bending, and friction at different levels of the multi-scale structure of the textile reinforcement. Friction can cause local defects such as wrinkling or yarn breakage, significantly altering the quality of the final product, and can modify the final orientation of the fibres, which is crucial for the mechanical behaviour of the composite part. Friction also plays a significant role in the cohesion and the deformation mechanism of a dry fibrous network. Consequently, understanding the friction behaviour between reinforcements is necessary so as to understand, master and optimize the first forming step in LCM processes. A growing number of studies have therefore been conducted on the friction behaviour between fibrous reinforcements or on the relationship between friction and formability [1, 2, 4-8]. However, since it is a complex issue due to the multi-scale fibrous nature of the reinforcements, considerable research remains to be done in order to fully understand e this phenomenon.

Different kinds of studies on the frictional behaviours of textile and technical reinforcements have been conducted over the past years. These materials are in general defined in terms of their multi-scale character: macroscopic (fabric), mesoscopic (tow or yarn) and microscopic (fibre). Studies carried out at each scale, using different devices, show that depending on the scale considered, the behaviour obtained appears to be different.

At the microscopic scale, Nowrouziah et al. evaluated experimentally and with a microscopic model the inter-fibre friction forces of cotton to study the fibre processing and the effect of these forces on the yarn behaviour [9, 10]. They found that the friction behaviour was correlated to the yarn strength and its irregularity (variation in the fibre section). The fibre with the highest friction coefficient produced more regular yarns. Analysis of the variance of the modelling results showed that inter-fibre friction was more sensitive to the normal load than to the velocity.

At the mesoscopic scale, the friction between various couples of materials such as tow/tow, tow/metal and tow/fabric has been studied on reinforcements made from different fibres (aramid, carbon and E-glass). The results demonstrated the significance of the relative orientation between the tows (parallel and perpendicular) on inter-tow friction for technical reinforcements [11, 12]. The contact model proposed by Cornelissen provides a physical

explanation for the experimentally observed orientation dependence in tow friction (tow/metal or inter-tow) [12, 13]. The mesoscopic frictional behaviour of carbon tows was explained by the microscopic constitution of the tow assuming a close packing of filaments which leads the normal load in a stationary tow to transfer from one layer of filaments to the layer beneath.

Some recent papers deal with fabric/fabric and fabric/metal friction at the macroscopic scale. Many of them deal with textile materials and focus on the effect of test conditions with the aim of improving the manufacturing process or adapting and functionalizing the final product (clothes). Ajayi studied the effect of the textile structure on its frictional properties by varying the yarn sett (number of yarns/cm) and the crimp while keeping the Tex and thickness constant [14]. The frictional properties increased by increasing the crimp (and thus the density), which was attributed to the knuckle effect of the textile. The term knuckle refers to the cross-over points of the warp and weft yarns making up the fabric. During the weaving process, knuckles generate yarn undulations, i.e. an irregular and rough surface of the fabric, because the two sets of yarns interlace with each other. The yarn undulation is characterised by the yarn knuckle, which is defined as the yarn crown.

Furthermore, several studies have been conducted to understand the effect of the test conditions, such as atmospheric conditions which are relevant for textiles used for clothing especially as they are often made of natural materials. Several parameters, such as relative humidity, fabric structure, type of fibre material and direction of motion were found to exhibit an effect on the textile/textile friction while temperature (0-50°C) did not significantly influence the frictional parameters [15]. Here again, the most significant parameter was related to the fabric structure. Das and co-workers [16] examined the textile/textile and textile/metal frictional characteristics that simulate interaction between clothing items and fabric movement over a hard surface. They performed frictional tests with different normal pressures on commercial fabrics typically used in clothing industries in which some are composed of 100% of the same material while others are blended (made with two materials such as polyester/cotton). It was concluded that fabric friction is affected by the rubbing direction, type of fibre, type of blend, blend proportion, fabric structure and crimp. Fabric/metal friction is less sensitive to the rubbing direction.

A few studies deal with the macroscopic frictional response of technical reinforcements. These materials have many similarities with the textile family but also differences such as material constitution, unit cell size and some of the mechanisms involved during their frictional

behaviour. A recent benchmark compared results obtained with different devices developed by teams working on this topic [6]. Experimental tests on fabric/metal friction performed by the different teams on Twintex reinforcement exhibited an effect of pressure and velocity on the dynamic friction coefficient. In another study, the fabric/fabric friction behaviour was characterized using a specific device on different glass and carbon fabric architectures [7]. It was shown that the fabric/fabric friction was highly different and more complex than that of textile or homogeneous materials. The measured values varied by up to a factor of two during the friction test under the same conditions. A period and an amplitude that depend strongly on the relative positioning and shift of the two samples characterize the frictional signal. The period of the signal can be directly related to the unit-cell length (periodic geometry). In addition, the specificity of the fabric/fabric contact behaviour was found to be directly related to the shocks taking place between overhanging yarns. However, no studies were found in the literature addressing the interesting question of the effect of test conditions that are representative of the preforming of dry reinforcements on fabric/fabric friction behaviour.

The study carried out by Cornelissen is undoubtedly useful to build a relationship between the micro and the meso scales as regards friction, but extensive experimental work needs to be performed at the meso and macro scales in order to obtain enough data for the correct definition and identification of a future model. It is therefore necessary to study the variation in friction behaviour with respect to the normal pressure and velocity for different fabric architectures to contribute to a better understanding of fabric/fabric friction behaviour. This is the goal of the present paper.

## **2. Materials and Methods**

### **Tested dry fabric**

The experiments were conducted on a glass plain weave dry fabric (figure 1.a). This balanced fabric has a thickness of 0.75 mm and an areal weight of 504 g/m<sup>2</sup>. The width of the yarn is 3.75mm and the average spacing between neighbouring yarns (for weft and warp directions) is around 5mm comprising 1.25mm of spacing because the yarns are not tightened together. The unit cell length is ~10 mm. For the tow samples, the yarns were extracted from the woven fabric.

### **Description of the device**

When undertaking experimental investigations of dry-fabric friction, the various mesoscopic heterogeneities, the different unit cell sizes and anisotropy should be considered. This requires the use of specific experimental equipment designed to consider these properties. A specific experimental device at the laboratory PRISME, presented in Figure 1.b, is dedicated to this task [17]. The device consists of two plane surfaces, on which the two samples are fixed, sliding relative to each other. The bottom sample is fixed on a rigidly and accurately guided steel plate that can be moved horizontally in a fixed direction. The imposed velocity can vary from 0 to 100 mm/s. The top sample is fixed on a steel plate which is linked to a load sensor connected to a data acquisition system used to record tangential forces during the test. A dead weight on the top sample provides a constant normal load  $F_N$ . To obtain a uniform pressure distribution on the contact area of the samples, a calibration procedure was performed before testing to determine the optimal position of the dead weight [17]. For fabric/fabric experiments, the position of the dead weight was defined by using the mean of the tangential force. This approach gives an average position which limits the effect of specimen misalignment.

### **Test conditions**

Before starting the experiments, the samples were conditioned in standard laboratory conditions ( $T \sim 23^\circ$ ,  $RH \sim 50\%$ ). To distinguish the different physical phenomena occurring during the friction tests, an acquisition frequency of 50Hz was used. This value was chosen based on tests performed in a previous study on the same material with the same bench. The friction coefficient ( $\mu$ ) was calculated using Coulomb's theory:

$$\mu = \frac{F_T}{F_N} = \frac{F_T}{M \cdot g} \quad (1)$$

where  $F_T$  is the tangential load measured by the sensor,  $F_N$  is the normal load,  $M$  is the total mass of the upper specimen with the dead weight and  $g$  is gravitational acceleration.

To investigate the effect of the shaping process conditions on both the macroscopic and mesoscopic behaviours of the fabric, two kinds of friction tests were performed: fabric/fabric and yarn/yarn. Tests were conducted in four relative positions of the samples, varying: pressure and test speed. For the relative positioning of the samples, four different orientations were tested:  $0^\circ/0^\circ$ ,  $0^\circ/90^\circ$ ,  $90^\circ/90^\circ$  and  $0^\circ/45^\circ$ . These configurations, generally used in laminates, exhibit extreme friction coefficients (maximum and minimum) of two fabric plies [7]. The

position  $0^\circ/0^\circ$  was the reference one, and consisted in orienting the weft yarns of the two samples in the stroke direction. For  $0^\circ/90^\circ$  and  $0^\circ/45^\circ$ , the lower sample was kept along the same direction as the reference configuration, while the upper sample was rotated. For the  $90^\circ/90^\circ$  configuration, the warp yarns of the two samples were oriented in the sliding direction. For the yarn samples, the  $0^\circ$  orientation corresponds to the tows oriented in the movement direction, while  $90^\circ$  means that they are perpendicular.

Tests were conducted at five different pressures (3, 5, 10, 20 and 50 kPa) that are in the range of values involved during dry fabric preforming and at a speed of 1 mm/s. This velocity is the one used in a previous study to investigate the effect of pressure on fabric/metal friction behaviour [6]. It is in the order of magnitude of inter-ply velocity values during the forming of dry reinforcements [1]. The pressure is calculated by dividing the normal force by the areal size of the upper specimen. This definition is even the same for the fabric/fabric and yarn/yarn tests. Indeed, each specimen (upper and lower) of yarn/yarn tests contain several yarns that were placed next to each other. Consequently, the calculated pressure for fabric/fabric tests will be a theoretical one and not a real one because the contact between the two samples will not occur on this whole surface due to crimp and nesting.

The velocity values selected were 0.1, 1, 10 and 50 mm/s. This gives us a factor of 500 between the lowest and highest speed which covers the inter-ply sliding speed range during multi-layer forming whatever the laminate considered [1]. The tests with different pressures were analysed to determine the pressure value at which the tests with various velocities were performed. This pressure was determined in order to distinguish the effect of the two parameters and make the comparison reliable.

At least five tests were performed for each test case.

### **3. Results and discussion**

#### **3.1. FABRIC/FABRIC FRICTION BEHAVIOUR**

Typical layer/layer friction behaviour for dry fabric is illustrated in figure 2. This curve shows very clearly that the fabric/fabric friction behaviour is very different from the Coulomb/Amonton friction behaviour of a homogeneous material. A previous study showed that this behaviour is due to the superposition of two phenomena [7]: yarn/yarn friction between the yarns of the two dry fabric plies, and shocks between the transverse overhanging yarns of each ply. During the weaving process, warp and weft yarns are manipulated in such a way that the two sets of yarns interlace with each other to create the required pattern of the fabric. The sequence in

which they interlace with each other is called the woven structure (meso-structure). The yarns of one direction are bent around their crossing neighbour yarns, generating different crimps of the two networks resulting from the asymmetry of the weaving process. As a result, a height difference is obtained between the weft and neighbouring warp which is defined as depth overhanging or knuckle height (see figure 3) which promotes the shock phenomenon (lateral compression of yarns). These shocks occur periodically and generate high tangential reaction forces (F) leading to a substantial increase in the maximum friction values. The periodicity of the shocks is linked to the fabric meso-architecture and the relative position of the plies since it is difficult to control the relative position of the two samples during the tests, especially for reinforcements that have a weak unit cell length. During the positioning of the two samples on each other before testing, one may obtain a configuration in which the two are perfectly superimposed (figure 4.a) or laterally shifted (figure 4.b). When the two plies are perfectly superimposed the peak period is associated to the length of the sample unit cell, which is  $\sim 10$  mm for the glass plain weave considered here. Figure 2 illustrates this configuration. On the other hand, when the plies are not perfectly superimposed (shifted samples), the peaks appear at periods equal to a portion (half in the case of the plain weave) of the fabric unit cell length.

In order to analyse the variation in the values of the fabric/fabric friction coefficient, the static frictional coefficient ( $\mu_s$ ) was first taken as the highest peak at the beginning of the motion (e.g. around 4 seconds in figure 2). After an area containing the maximum peak (20 seconds on figure 2), the dynamic friction domain can be considered as established. The dynamic friction coefficient ( $\mu_k$ ) can then be associated to the average of all the measured values. Moreover, the maximum values of the dynamic friction (peaks) and minimum values (valleys) were measured in order to assess the effect of the test conditions on the shock phenomenon. Maximum and minimum friction coefficients are noted respectively  $\mu_{\max i}$  and  $\mu_{\min i}$ . The mean and standard deviation ( $\sigma$ ) of each are calculated. These measurements were only considered for friction tests in which the period was close to the length of the unit cell for the configurations  $0^\circ/0^\circ$ ,  $0^\circ/90^\circ$  and  $90^\circ/90^\circ$ . For  $0^\circ/45^\circ$ , as it is difficult to distinguish the unit cell length in the signal, all the peaks and valleys were considered to calculate  $\mu_{\max i}$  and  $\mu_{\min i}$ .

### Effect of Normal Pressure

The first test parameter considered in this study was the normal pressure. Fabric/fabric friction experiments were conducted at five pressures: 3, 5, 10, 20 and 50 kPa. The results of the static friction coefficients ( $\mu_s$ ) and the mean values of the dynamic friction coefficients ( $\mu_k$ ) are



presented in Table 1 and illustrated on figure 5 and figure 6. The results of the maximum values of the dynamic friction (measured at the peaks of the signal) and minimum values (measured at the valleys) are illustrated on figure 7. The error bars represent the standard deviations ( $\sigma$ ).

It can be seen that the fabric/fabric static friction coefficients were higher than the dynamic coefficients in all the test configurations (Table 1) and had slightly higher standard deviations. This is a common observation in friction responses, which has also been noticed on textiles [14, 16]. Furthermore, the relative orientation of the two specimens has an effect on the frictional behaviour. In all cases, the static and dynamic frictional coefficients were higher for the  $0^\circ/0^\circ$  configuration than for the  $90^\circ/90^\circ$  configuration (Figure 5, Figure 6 and figure 7). The same trend has been observed on other fabric architectures, such as carbon interlock [7], and can be attributed to the weaving effect (difference in crimp between the two yarn networks). As already mentioned, the fabric/fabric friction behaviour is governed by yarn/yarn friction and shocks between overhanging transverse yarns. The friction coefficient varied hugely (by up to a factor of two) because of high tangential forces due to the second phenomenon which predominates the global friction behaviour. According to the measures obtained, the tangential reaction forces due to shocks between weft yarns (configuration  $0^\circ/0^\circ$ ) are higher than those between warp yarns (configuration  $90^\circ/90^\circ$ ). As the reinforcement is assumed to be balanced and networks (weft and warp) are composed of the same yarns, this can be explained by the difference in crimp between the two networks resulting from the asymmetry of the weaving process. To confirm this fact, the crimp of warp and weft yarns was measured according to the ASTM D3883-04 standard [18]. The crimp obtained for warp and weft yarns were respectively 0.35% and 0.43% confirming that higher crimp leads to higher tangential reaction forces due to yarn shocks. The increase in crimp results in a higher overhanging of the more crimped network yarn and thus in an increase of the friction coefficient. This conclusion is in good agreement with the study by Ajayi [13] which showed that an increase in the weft yarn density generated an increase in the frictional resistance of textile.

For the  $0^\circ/90^\circ$  configuration, transverse yarns are warp yarns (with high overhang value) for the bottom sample and weft yarns (with a low overhang value) for the upper sample. The shock phenomenon occurs between warp yarns that have high crimp and weft yarns with low crimp. As a result, the tangential forces obtained in this configuration and thus the friction coefficients remain in between those obtained in the  $0^\circ/0^\circ$  and  $90^\circ/90^\circ$  configurations (figure 5, figure 6 and figure 7). There are still some points for which this trend was not confirmed (e.g. 3 kPa and 5

kPa), especially for maximum and minimum friction coefficients (figure 7), which may be due to the imperfect superimposition of the two samples.

As expected, the lowest friction coefficients were obtained for the configuration  $0^\circ/45^\circ$  (see figures 5, 6 and tables 1 and 2). The measured signal of the tangential force was smoother than the other configurations (figure 8). The amplitude of the signal was very weak (figures 7 and figure 8), which means that shocks between the overhanging yarns were not severe. In fact, Shocks occurred between network of yarns, one of which was oriented at  $45^\circ$ , which led to a very weak instantaneous lateral contact width between yarns. As a result, the yarn/yarn friction in this configuration governed the frictional behaviour and consequently the measured dynamic coefficient was closer to that of the yarn/yarn at  $0^\circ/90^\circ$  (see section 3.2). When the normal pressure increased, the static and dynamic friction coefficients decreased (figure 5 and figure 6). This observation is in agreement with the results obtained for fabric/metal tests [6]. For the four configurations ( $0^\circ/0^\circ$ ,  $0^\circ/90^\circ$ ,  $90^\circ/90^\circ$  and  $0^\circ/45^\circ$ ), friction coefficients significantly decreased in the pressure range of 3-20 kPa before converging to a steady value whatever the test configuration (figure 5, figure 6 and figure 7). The only singular point is the friction behaviour at  $0^\circ/90^\circ$ , for which the maximum coefficient ( $\mu_{\max}$ ) measured at a pressure of 5 kPa was higher than that measured at 3 kPa. This has an impact on the static and dynamic coefficient values, which show the same trend. This can be attributed to the low pressure. At this level of pressure (3 kPa), the shock phenomenon is not the predominant one and the behaviour is dominated by yarn/yarn friction. Thus, at this level of pressure, the friction behaviour tends closer to that of the  $90^\circ/90^\circ$  configuration. This point will be addressed in future work.

After a pressure of 20 kPa, the fabric/fabric friction behaviours levelled off. Thus, the static ( $\mu_s$ ) and dynamic ( $\mu_k$ ) coefficients reached stabilized values with a low standard deviation, which denotes the good reproducibility of these behaviours (Table 1). The maximum decrease was obtained for the  $0^\circ/0^\circ$  configuration (around 30% for the static and dynamic coefficients) while in the  $0^\circ/45^\circ$  configuration only a 7% and 11% decrease was respectively observed for  $\mu_s$  and  $\mu_k$ .

This decrease in the friction coefficients can be attributed to the effect of fabric compaction and its consequences at the mesoscopic and macroscopic levels. When the pressure increases, the upper sample exerts a greater compaction on the lower. This leads to a high transverse compression strain of the fabric inducing at the mesoscopic level a reduction of the yarn's overhang height and a spreading of the yarns. At the macroscopic level, the reduction in the

thickness of the reinforcement can potentially lead to a lateral spreading of the fabric in the in-plane directions, and therefore a decrease in crimp. As the crimp at these stress states decreases, the texture ("roughness") of the fabric related to its meso-architecture decreases, and the contact area increases. However, the real contact area between the two samples driving the effective pressure is difficult to quantify for fabric/fabric friction tests (due to nesting, for example) in contrast to fabric/metal [19].

The reduction in yarn's overhang height due to compaction leads to the decrease of the tangential reaction forces between the transverse yarns of the samples. As a result, the maximum friction coefficient ( $\mu_{\max}$ ), measured on the peaks of the curves, decreased (figure 7). In addition, the yarn spreading associated with the decrease in their overhang height generated a lower fabric "roughness". Therefore, the tangential reaction forces' signal, due to this new "roughness", was also smoother as observed for the 50 kPa pressure, while below 20 kPa the rise and fall in forces at each peak were more pronounced and abrupt (figure 9). It can also be seen that the maximum friction coefficient  $\mu_{\max}$  continued to decrease slightly and was not completely stable at 50 kPa (figure 7), except for the configuration 0°/45° where the shocks phenomenon has a weak effect. Stabilization would probably occur at almost no meso roughness, which might be achieved at very high pressure not encountered during the composite shaping process.

The minimum friction coefficient ( $\mu_{\min}$ ) measured in the curve valleys, which is attributed to yarn/yarn friction [7], was not affected by this phenomenon and its evolution followed the same trend as the global friction behaviour (figure 7).

#### Effect of Velocity

In order to evaluate the effect of the sliding velocity on the fabric/fabric frictional behaviour, tests were conducted at four velocities: 0.1, 1, 10 and 50mm/s. These tests were performed at a pressure of 35 kPa as the friction behaviour versus pressure is stabilized at this pressure. It was previously observed that the friction coefficients at 0°/90° were situated between those of the 0°/0° and 90°/90° configurations and generally close to the 0°/0° configuration. For this reason, only the 0°/0°, 0°/45° and 90°/90° configurations were tested here. The static and dynamic friction coefficients obtained are summarized in table 2. The coefficients were measured with a good reproducibility (maximum deviation of 12% for the dynamic coefficient).

The friction coefficients changed slightly regardless of the configuration tested. The static friction coefficient increased from 0.427 to 0.503 when the velocity increased from 0.1 to 50

mm/s in the 0°/0° orientation, an increase of approximately 17 % (figure 10). On the other hand, the 90°/90° configuration was less sensitive to the velocity with a maximum decrease of 9% at 50 mm/s compared to 0.1mm/s, which remains in the order of magnitude of experimental deviations. Once again, the 0°/0° configuration was more sensitive to the test parameters, which is likely due to its high crimp and therefore the predominance of the shock phenomenon.

The same trend was observed for the dynamic friction coefficients but to a lesser extent. The coefficients increases between 9 % and 14 % for all the configurations (figure 10). This slight increase in the dynamic friction is essentially due to the contribution of the minimum friction ( $\mu_{\min}$ ) coefficient while the maximum ( $\mu_{\max}$ ) decreased as can be observed on figure 11. Consequently, increasing the speed has more influence on the amplitude variation than on the average value. Increasing the speed leads to an increase in the frequency of shocks which has two consequences:

- The kinetic energy of the yarns (of the lower sample) enables them to pass over the overhanging transverse yarns in a shorter time with a lower force. The maximum friction coefficient therefore decreases. This also causes an up and down movement of the upper sample that can be described as stick-slip phenomenon.
- Between two shocks, a steady sliding between yarns does not exist, consequently the tangential force does not reach the stabilized value tending towards the friction coefficient of the yarns. Accordingly, the minimum coefficient increases.

For the configuration 0°/45°, both coefficients ( $\mu_{\max}$  and  $\mu_{\min}$ ) increased. As, it has been discussed previously, these values are given in this configuration for information only and are not related to the meso-architecture in which case the values would have been different. Therefore, they cannot be used for comparison with other configurations.

To summarize, as the velocity increases, the upper sample does not follow strictly the irregularities of the lower sample which leads to a decrease in the signal variation just as if the irregularities were lower. It can be concluded that at low velocities (0.1 to 1mm/s) the dynamic frictional coefficient can be considered as almost constant whatever the orientation while beyond a velocity of 1 mm/s, its evolution as a function of the velocity should be considered.

### **3.2. YARN/YARN FRICTION BEHAVIOUR**

The second aim of this study was to determine the effect of the test parameters on the friction behaviour at the mesoscopic level. Yarn/yarn friction tests were therefore conducted, varying

the pressure and the velocity. Only the  $0^\circ/0^\circ$  (parallel case) and  $0^\circ/90^\circ$  (perpendicular case) configurations were performed. Recall that the  $0^\circ$  orientation means that the yarns are oriented in the direction of the stroke and  $90^\circ$  in the transverse direction.

#### Effect of Normal Pressure

As in the fabric tests, yarn/yarn friction tests were conducted by varying the normal pressure at 1mm/s. The results of the static ( $\mu_s$ ) and dynamic ( $\mu_k$ ) friction coefficients are summarized in table 3 and illustrated on figure 12 and figure 13. As expected, the static friction coefficients and their standard deviations were higher than for the dynamic coefficients. Moreover, the friction values were greater at  $0^\circ/0^\circ$  than at  $0^\circ/90^\circ$  which is in good agreement with previous studies carried out on carbon, aramid and glass yarns [11, 12].

The friction behaviour for the perpendicular configuration is mainly controlled by inter-fibre friction while for the parallel case, other phenomena are involved, among which: fibre bending, fibre reorganisation in the yarns, transverse compression, fibre damage, intermingling of fibres between yarns, etc. These phenomena are promoted by the spinning process, because fibres do not remain straight and some of them are damaged like it can be seen on figure 14. This generates reaction forces during tests that lead to the increase in friction forces. When the pressure increased, the static and dynamic coefficients decreased before reaching a plateau beyond 10 kPa. The decrease was larger in the parallel case ( $0^\circ/0^\circ$  configuration) with respect to the perpendicular one ( $0^\circ/90^\circ$ ). For high pressure (50kPa), the friction increase because the higher compression rate generates more fibre damage. This fact is illustrated on Figure 15 showing the results where the friction coefficient increases after stabilization (beyond 40 s). Observations performed using a microscope on this sample after the test showed a large number of broken fibres.

#### Effect of Velocity

The friction tests according to velocity were performed under 35 kPa as for the fabric/fabric tests. The results are summarized in table 4 and illustrated in figure 16. Once again, it was observed that the static friction coefficient was higher than the dynamic one.

As for fabric/fabric, the tow/tow friction behaviour remained unchanged in the range 0.1-1 mm/s velocities whatever the relative position of the samples. The friction was still constant for the parallel yarns ( $0^\circ/0^\circ$ ) while for the perpendicular ( $0^\circ/90^\circ$ ) case, an increase of more than 43% in the friction coefficient values was observed with the increasing velocity. It can be concluded

that while the velocity does not affect the phenomena (intermingling of fibres between yarns, fibre reorganisation in the yarns, bending, etc.) controlling inter-tow friction in parallel yarns, it significantly affects the response for the  $0^\circ/90^\circ$  configuration which is mainly controlled by inter-fibre friction. This trend is very different from the one observed on natural cotton fibres, which are more sensitive to pressure than to speed [9, 10]. The differences between these fibres and those used in the present study (glass) are mainly related to their mechanical behaviour (brittle vs ductile), their compressibility and roughness. These characteristics are highly correlated with the friction coefficient [9]. As a conclusion, the fibre material significantly influences the effect of the test conditions on the microscopic friction behaviour (fibre/fibre) which results in the same effect at the mesoscopic level (yarn/yarn).

#### **4. CONCLUSIONS**

This study has highlighted the influence of test conditions on the frictional behaviour of dry reinforcements at mesoscopic and macroscopic scales. It was found that the friction behaviour depends strongly on the relative orientation of the samples. Furthermore, experimental tests performed at the macroscopic level (fabric/fabric) showed that, for a given yarn, the friction coefficient is highly related to the yarn crimp because of the shock phenomenon occurring between transverse overhanging yarns. Friction coefficients decrease when the normal pressure increases until reaching steady values, which are almost identical whatever the relative orientation of the specimens. The greater decrease observed for the  $0^\circ/0^\circ$  configuration can be attributed to the effect of the fabric compaction and its consequences on the yarn and fabric structure, i.e. a decrease in the yarn's overhang height and yarn spreading leading to the decrease in crimp.

Velocity has the opposite effect on fabric/fabric friction since the coefficients increase with the velocity. The static friction coefficient and the  $0^\circ/0^\circ$  configuration are more sensitive to this parameter. The dynamic friction coefficient remains almost unchanged at low velocities whatever the relative orientation of the two samples while it increases slightly for high speeds. This increase is due to the contribution of the minimum friction coefficient ( $\mu_{\min}$ ) that increases because the high frequency between two shocks does not permit a stabilization of the tangential force at values tending towards the friction coefficient between yarns. However, the main effect of high speeds is a finite decrease in the amplitude variation of the friction response.

At the mesoscopic level, the results show the same trend as for macroscopic friction as a function of the test parameters. The parallel configuration  $0^\circ/0^\circ$  is more sensitive to pressure while the  $0^\circ/90^\circ$  is more influenced by velocity. This is due to the fact that friction behaviour in the perpendicular configuration is mainly controlled by inter-fibre friction while for the parallel case, other phenomena promoted by the spinning process are involved. It has been shown that the material constituting the fibres mainly influences the effect of the test conditions on the microscopic friction behaviour (fibre/fibre) which results in the same effect at the mesoscopic level (yarn/yarn).

We can conclude that at each scale, the frictional behaviour of the material studied here, which is heterogeneous and multiscale (micro-meso-macro), is governed by friction but is also significantly influenced by the structure of the lower scale. These structures (meso, micro) reorganise when test conditions such as pressure are varied, which leads to a variation in the friction behaviour. Thus, even if the same trends of the effect of test conditions are observed at different scales (meso, macro), they are caused by different mechanisms which are due to the structural reorganization at the lower scale.

### **Acknowledgments**

The research leading to these results received funding from the Mexican National Council of Science and Technology (CONACyT) under grant no I0010-2014-01.

### **References**

- [1] Allaoui S., Cellard C., Hivet G. Effect of inter-ply sliding on the quality of multilayer interlock dry fabric preforms. *Composites Part A*, 2015; 68:336-345.
- [2] Ten Thije RHW, Akkerman A. A multi-layer triangular membrane finite element for the forming simulation of laminated composites. *Composites Part A*, 2009; 40:739-53.
- [3] Hivet G., Allaoui S., Soulat D., Wendling A., Chatel S. Analysis of woven reinforcement preforming using an experimental approach. *Proceedings of the 17th International Conference on Composite Materials*, Edinburgh, UK, July, 2009.
- [4] Hamila N., Boisse P. Simulations of textile composite reinforcement draping using a new semi-discrete three node finite element. *Composites Part B*, 2008; 39:999-1010.
- [5] Gorczyca-Cole J.L., Sherwood J.A., Chen J. A friction model for thermostamping commingled glass-polypropylene woven fabrics. *Composites Part A*, 2007; 38(2): 393-406.

- [6] Sachs U., Akkerman R., Fetfatsidis K., Vidal-Sallé E., Schumacher J., Ziegmann G., Allaoui S., Hivet G., Maron B., Vanclooster K., Lomov S.V. Characterization of the dynamic friction of woven fabrics: Experimental methods and Benchmark results. *Composites Part A*, 2014; 67:289-298 .
- [7] Allaoui S., Hivet G., Wendling A., Ouagne P., Soulat D. Influence of the dry woven fabrics meso-structure on fabric/fabric contact behaviour. *Journal of Composite Materials*, 2012; 46(6): 627-639.
- [8] Ten Thije RHW, Akkerman R. Design of an experimental setup to measure tool-ply and ply-ply friction in thermoplastic laminates. *Int J Mater Form* 2009; 2(1): 197–200.
- [9] Nowrouzieh S., Drean J.Y., Sinoimeri A. The investigation of frictional coefficient for different cotton varieties". *Applied Science Reports*. 2013; 3(2):116-120.
- [10] Nowrouzieh S., Sinoimeri A., Dréan J.Y., Frydrych R., Gurlot J.P. Inter fiber frictional model. *Research Journal of Textile and Apparel*, 2007; 11 (4): 64-70.
- [11] Vidal-Sallé E., Massi F. Friction Measurement on Dry Fabric for Forming Simulation of Composite Reinforcement. *Key Engineering Materials*." 2012; 504-506:319-324.
- [12] Cornelissen B., Rietman B., Akkerman R. Frictional behaviour of high performance fibrous tows: Friction experiments. *Composites: Part A*, 2013; 44:95–104.
- [13] Cornelissen B., De Rooij M.B., Rietman B., Akkerman R. Frictional behaviour of high performance fibrous tows: A contact mechanics model of tow–metal friction. *Wear*, 2013; 305(1-2):78-88.
- [14] Ajayi J.O. Effects of fabric structure on frictional properties. *Textile Research Journal*, 1992; 62(2): 87-93.
- [15] Arshi A., Jeddi Ali A.A., Moghadam M.B. Modeling and optimizing the frictional behavior of woven fabrics in climatic conditions using response surface methodology. *The Journal of the Textile Institute*, 2012; 103(4):356-369
- [16] Das A., Kothari V. K., Vandana N. A study on frictional characteristics of woven fabrics. *AUTEX Research Journal*, 2005; 5(3):133-140.
- [17] Hivet G., Allaoui S., Cam B.T., Ouagne P., Soulat D. Design and potentiality of an apparatus for measuring yarn/yarn and fabric/fabric friction. *Experimental Mechanics*, 2012; 52 (8): 1123-1136.



- [18] ASTM D3883-04 Standard Test Method for Yarn Crimp and Yarn Take-up in Woven Fabrics. 2011.
- [19] Cornelissen B., Sachs U., Rietman B., Akkerman R. Dry friction characterisation of carbon fibre tow and satin weave fabric for composite applications. *Composites: Part A*, 2014; 56:127–135.

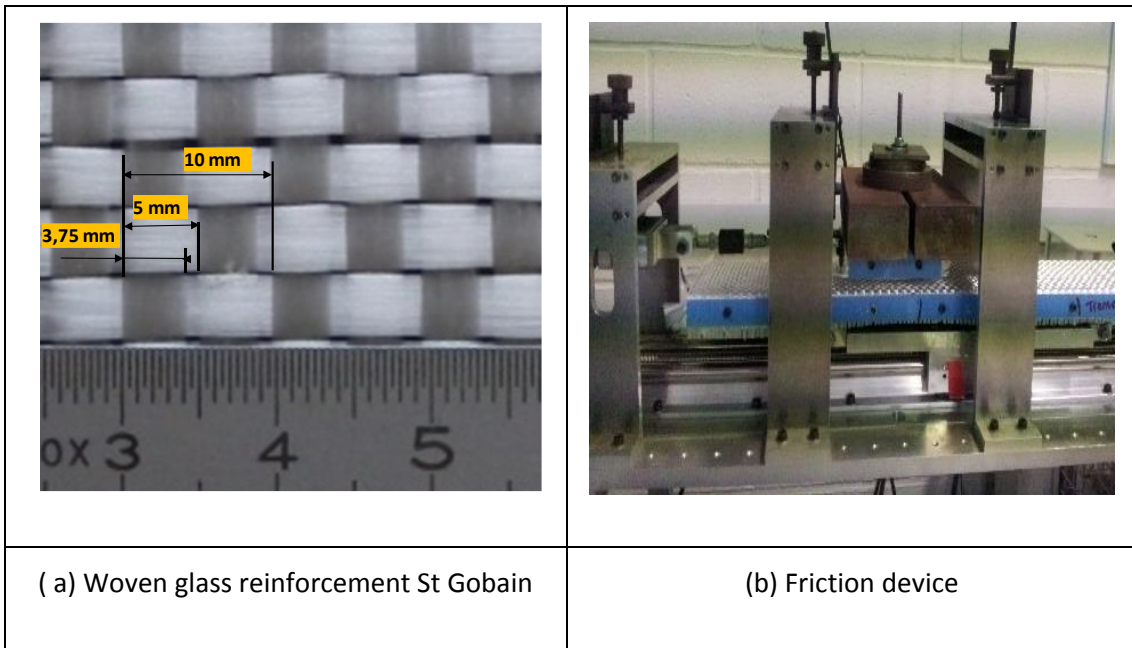


Figure 1. Material and equipment of the study

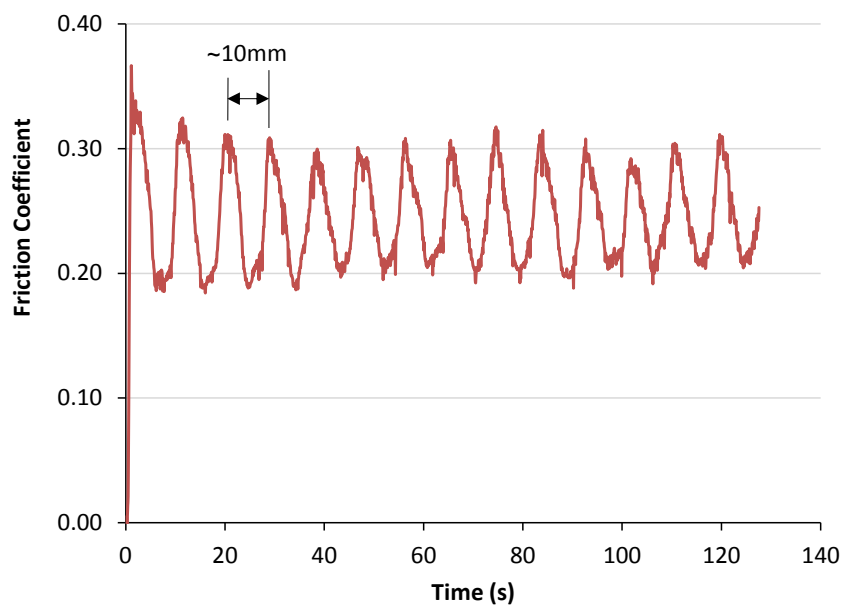


Figure 2. Typical fabric/fabric friction behavior for glass plain weave at pressure of 20 kPa and speed of 1 mm/s

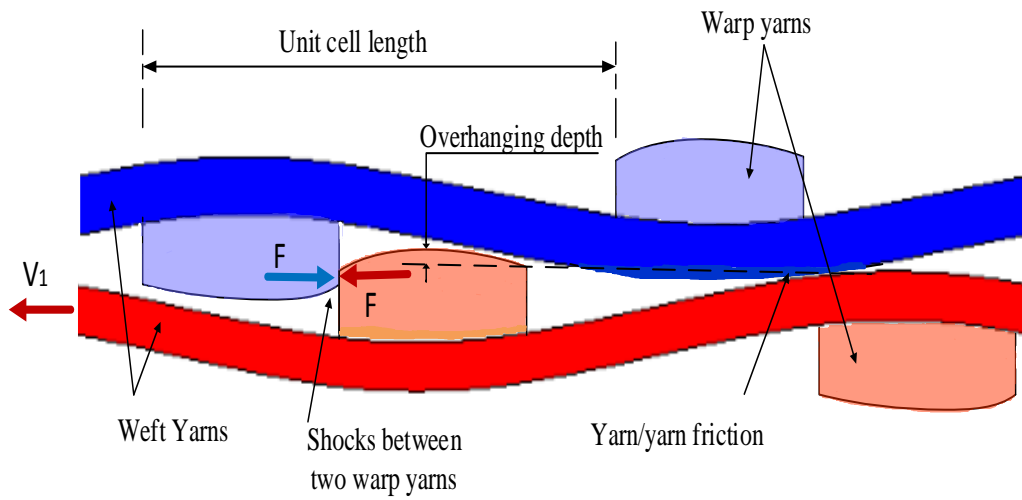


Figure 3: Phenomena occurring during fabric/fabric friction: yarn/yarn friction and shock phenomenon caused by overhanging yarns [1]

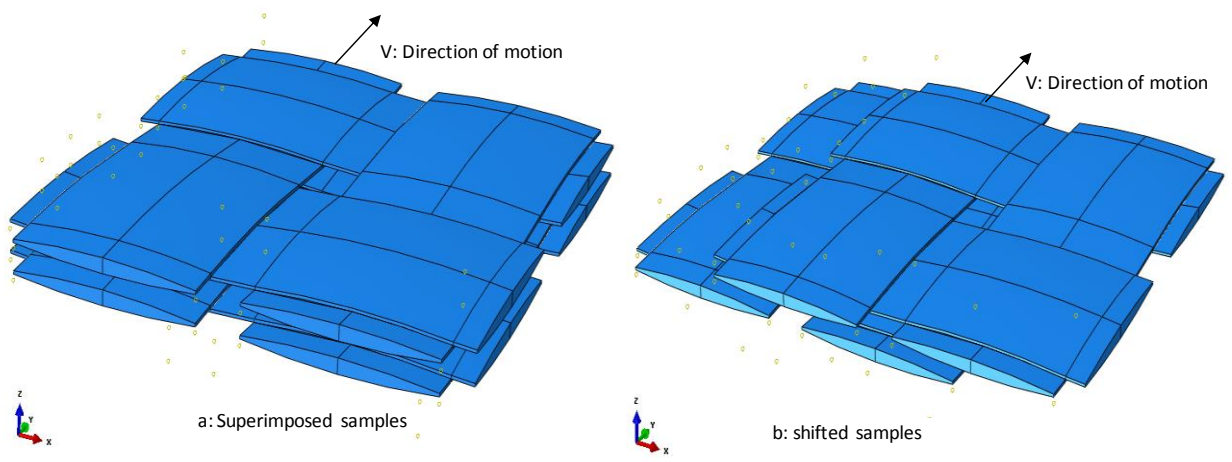


Figure 4: Relative positioning of the samples

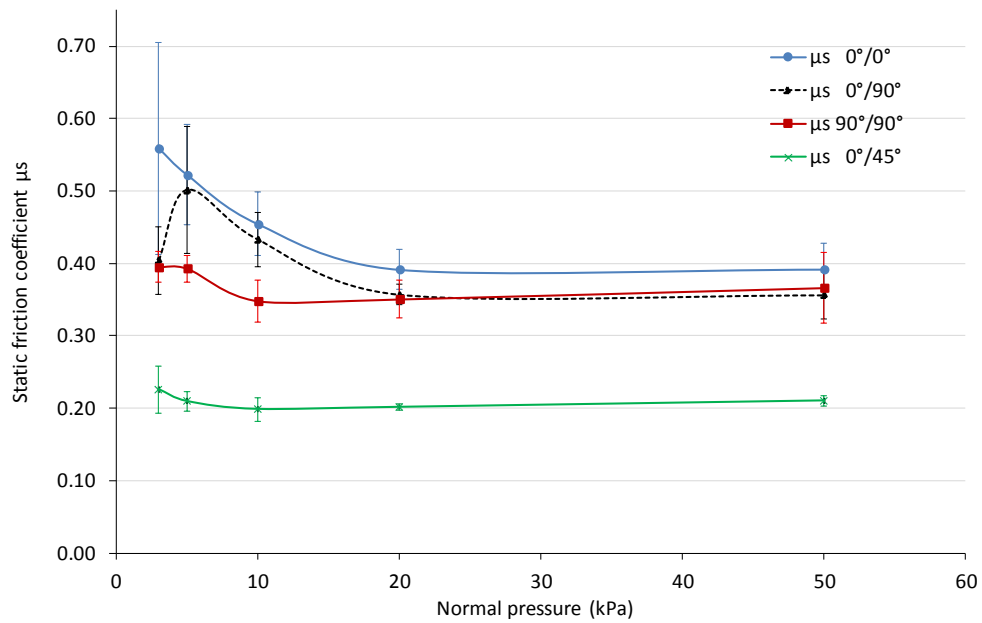


Figure 5. Evolution of Fabric/fabric static friction coefficient ( $\mu_s$ ) as a function of the normal pressure at velocity of 1mm/s. The error bars represent the standard deviations

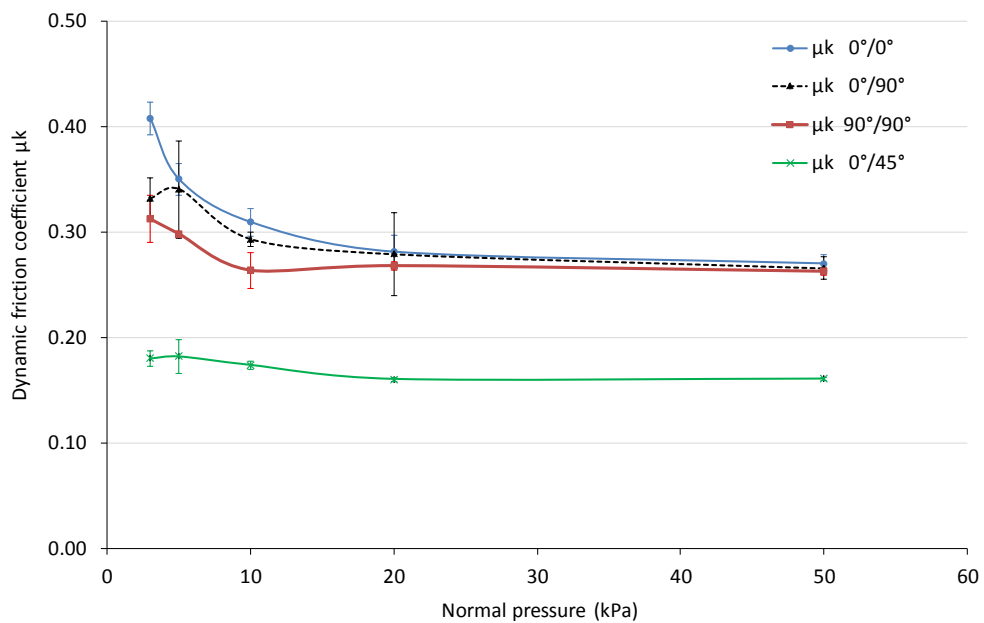


Figure 6. Evolution of Fabric/fabric dynamic friction coefficient ( $\mu_k$ ) as a function of the normal pressure at velocity of 1mm/s. The error bars represent the standard deviations.

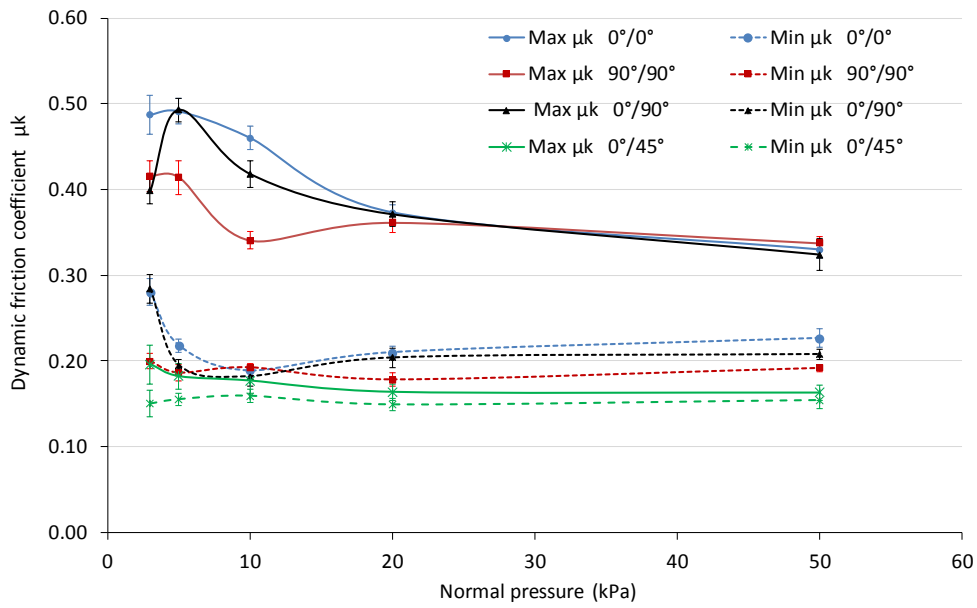


Figure 7. Evolution of the maximal ( $\mu_{\max}$ ) and minimal ( $\mu_{\min}$ ) values of the dynamic friction coefficient for fabric/fabric according to normal pressure. [Velocity of 1mm/s](#). The error bars represent the standard deviations

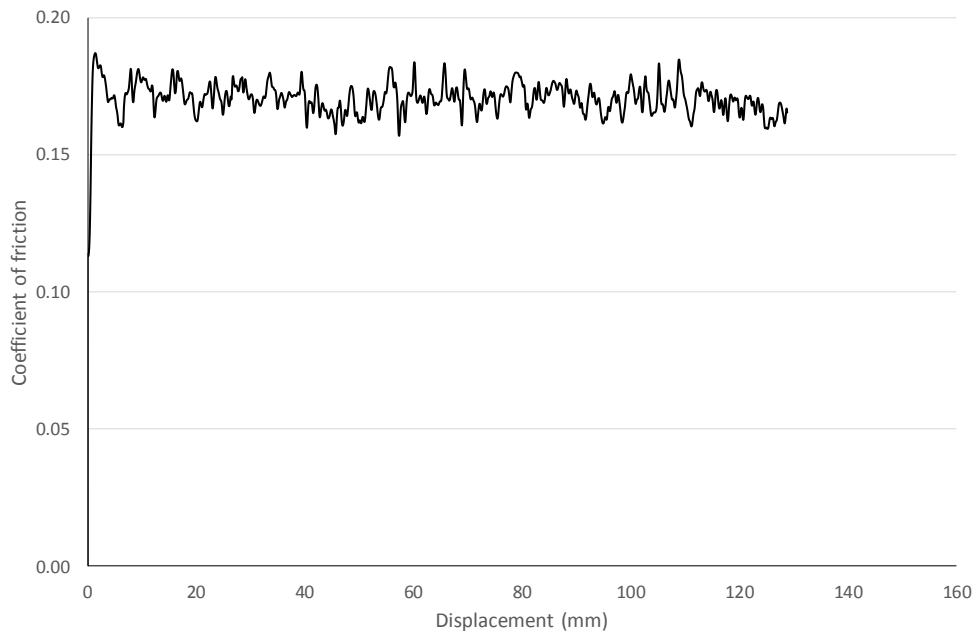


Figure 8. Frictional curve of the configuration  $0^\circ/45^\circ$  at test conditions of 10kPa and 1mm/s

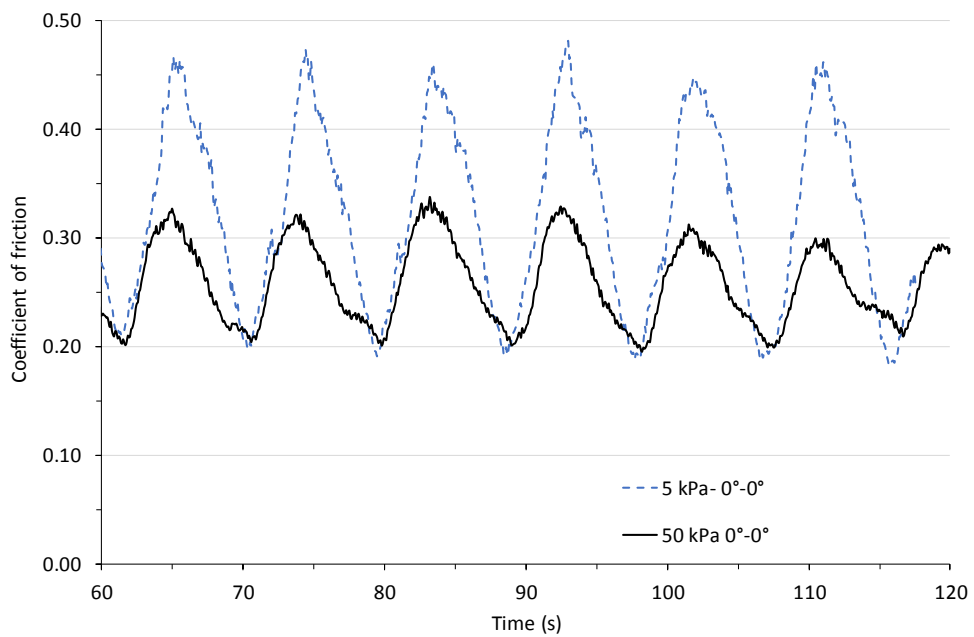


Figure 9. Comparison of the frictional behavior at pressures of 50 kPa and 5 kPa (configuration of  $0^\circ/0^\circ$ )

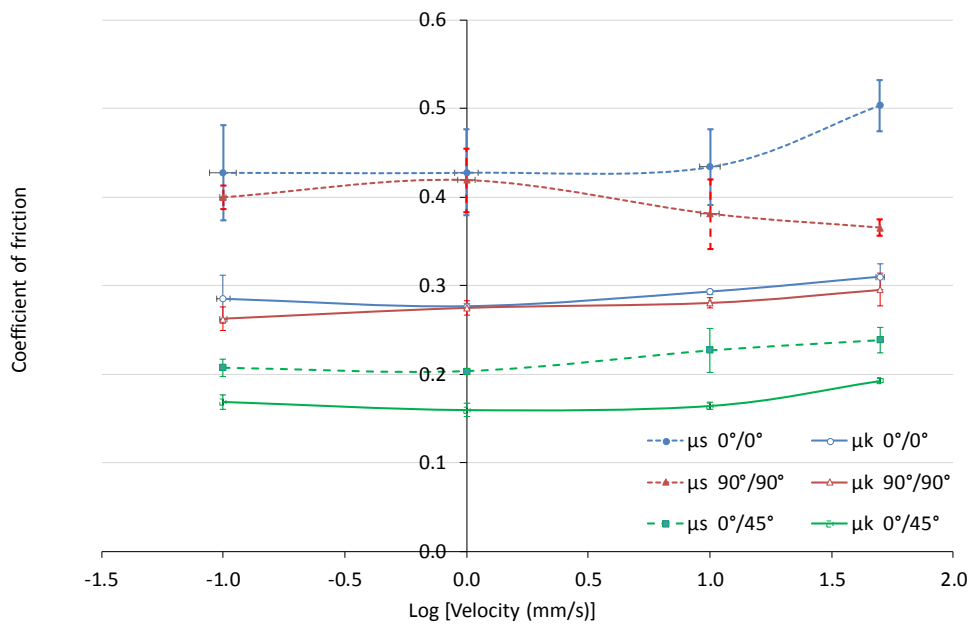


Figure 10. Evolution of static ( $\mu_s$ ) and dynamic ( $\mu_k$ ) of fabric/fabric frictional coefficients according to velocity at pressure of 35kPa. The error bars represent the standard deviations

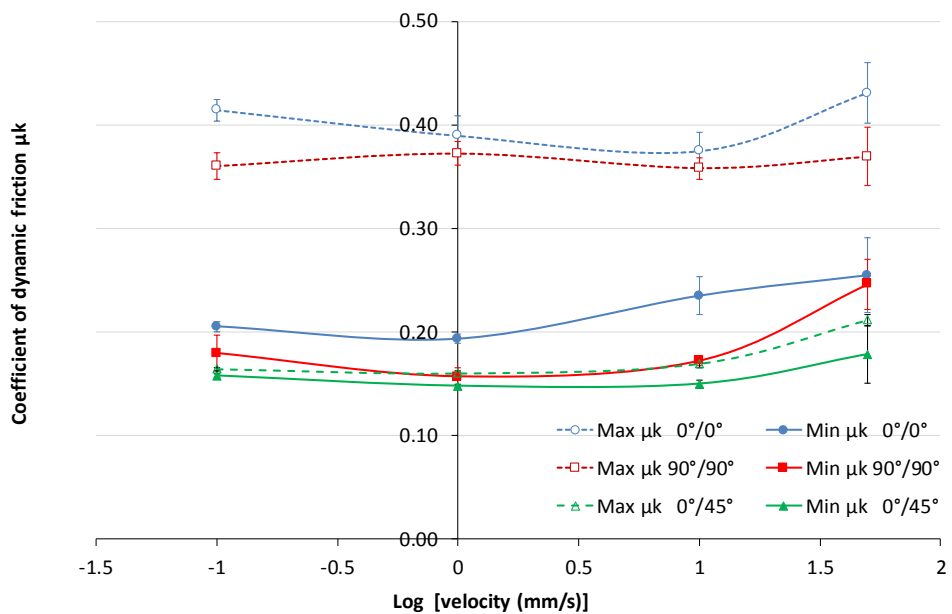


Figure 11. Maximum ( $\mu_{maxi}$ ) and minimum ( $\mu_{mini}$ ) friction coefficient versus velocity for the fabric/fabric. Pressure of 35kPa. The error bars represent the standard deviations

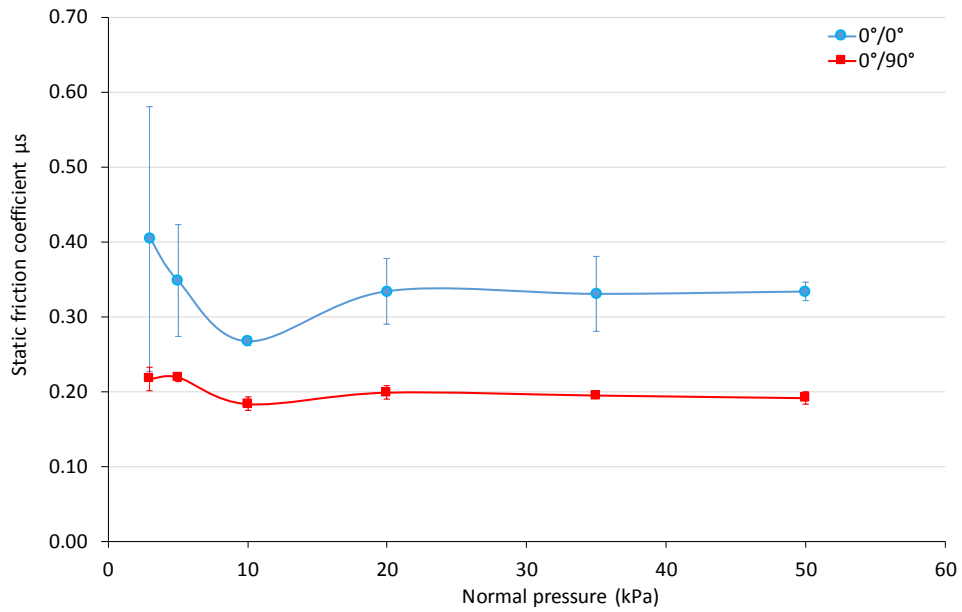


Figure 12. Static friction coefficient ( $\mu_s$ ) as function of the normal pressure for yarns/yarn tests at velocity of 1mm/s. The error bars represent the standard deviations

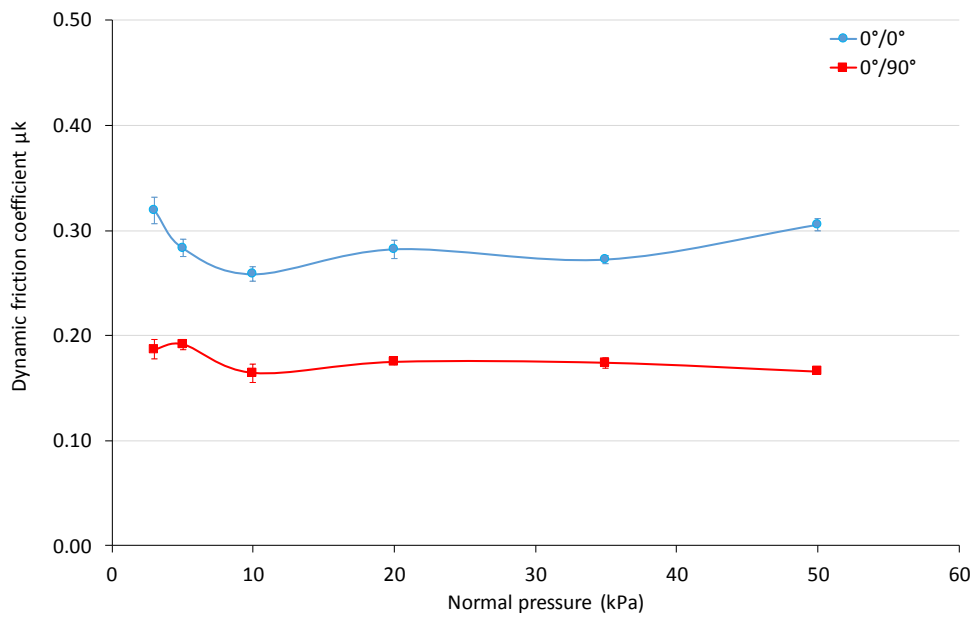


Figure 13. Dynamic friction coefficient ( $\mu_k$ ) as function of the normal pressure for yarns/yarn tests at velocity of 1mm/s. The error bars represent the standard deviations



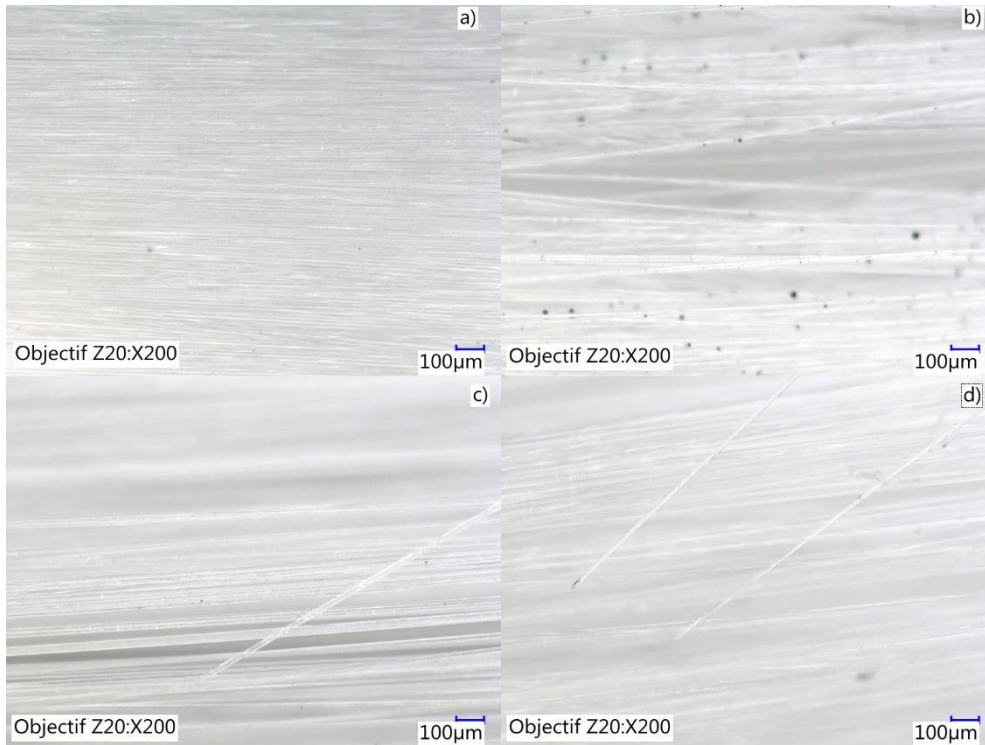


Figure 14. Microscopic observations of a non-tested yarn sample: a) global view; b) non straight and bended fibers; c) and d) damaged fibers.

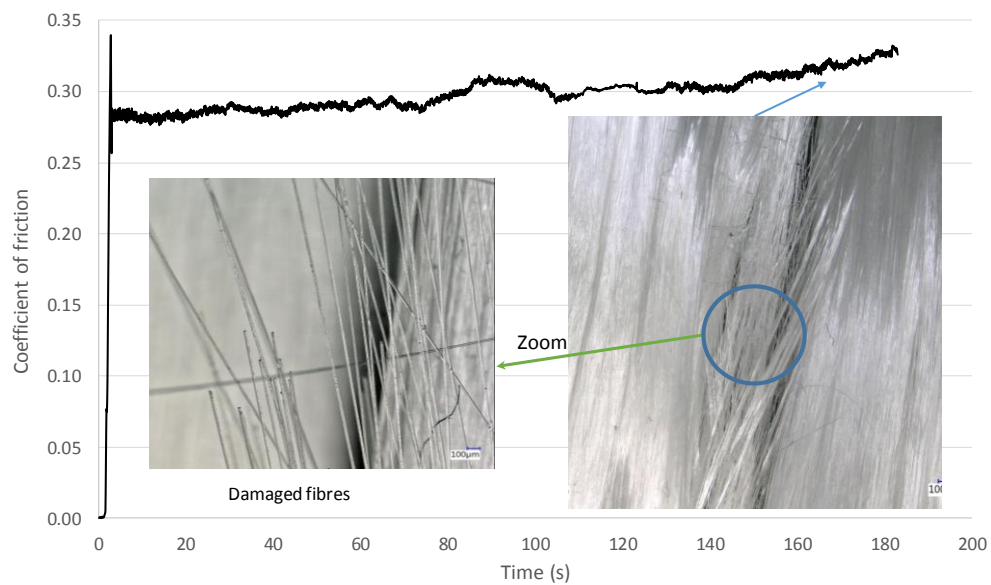


Figure 15. Effect of damaged fibre on the yarn/yarn frictional behaviour. Configuration 0°/0° at 50kPa.

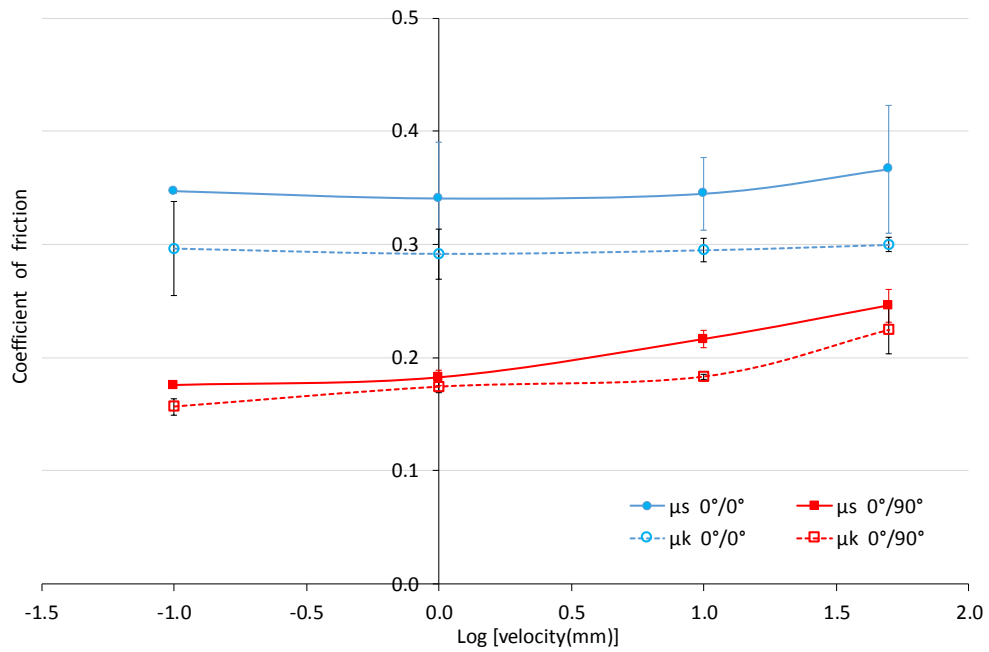


Figure 16. Evolution of yarn/yarn friction coefficients according to testing velocity at pressure of 35kPa. The error bars represent the standard deviations

Table 1. Fabric/fabric frictional characteristics function of the normal pressure at 1mm/s.

Orientation	Normal pressure (kPa)	$\mu_s$	Standard deviation [ $\sigma$ ]	$[\sigma/\mu_s]*100$ (%)	$\mu_k$	Standard deviation [ $\sigma$ ]	$[\sigma/\mu_k]*100$ (%)
0°/0°	3	0.5590	0.1461	26.13	0.4074	0.0155	3.80
	5	0.5224	0.0690	13.21	0.3499	0.0148	4.22
	10	0.4543	0.0442	9.72	0.3092	0.0131	4.23
	20	0.3911	0.0276	7.06	0.2810	0.0162	5.78
	50	0.3915	0.0339	8.65	0.2698	0.0120	4.45
0°/90°	3	0.4041	0.0467	11.55	0.3315	0.0198	5.98
	5	0.5012	0.0878	17.51	0.3401	0.0461	13.54
	10	0.4327	0.0375	8.66	0.2931	0.0067	2.30
	20	0.3566	0.0142	3.97	0.2789	0.0396	14.20
	50	0.3558	0.0320	9.00	0.2656	0.0107	4.02
90°/90°	3	0.3950	0.0210	5.33	0.3123	0.0223	7.12
	5	0.3928	0.0705	17.94	0.2982	0.0030	1.02
	10	0.3479	0.0287	8.25	0.2635	0.0167	6.34
	20	0.3504	0.0158	4.51	0.2678	0.0042	1.58
	50	0.3661	0.0354	9.67	0.2625	0.0062	2.35
0°/45°	3	0.2256	0.0320	14.18	0.1799	0.0070	3.90
	5	0.2093	0.0133	6.35	0.1818	0.0159	8.75
	10	0.1985	0.0162	8.14	0.1737	0.0039	2.27
	20	0.2014	0.0040	1.99	0.1602	0.0019	1.17
	50	0.2102	0.0073	3.49	0.1605	0.0012	0.75

Table 2. Experimental friction coefficients of fabric/fabric at 35 kPa\_according to velocity

Orientation	Velocity (mm/s)	Log [velocity]	$\mu_s$	Standard deviation [ $\sigma$ ]	$[\sigma/\mu_s]*100$ (%)	$\mu_k$	Standard deviation [ $\sigma$ ]	$[\sigma/\mu_k]*100$ (%)
0°/0°	0.1	-1.0	0.4274	0.0541	12.65	0.2846	0.0269	9.46
	1.0	0.0	0.4275	0.0484	11.31	0.2760	0.0032	1.17
	10.0	1.0	0.4338	0.0424	9.78	0.2928	0.0031	1.07
	50.0	1.7	0.5031	0.0289	5.75	0.3098	0.0149	4.82
90°/90°	0.1	-1.0	0.3993	0.0130	3.25	0.2623	0.0136	5.20
	1.0	0.0	0.4186	0.0358	8.55	0.2746	0.0084	3.06
	10.0	1.0	0.3809	0.0394	10.33	0.2802	0.0057	2.03
	50.0	1.7	0.3652	0.0089	2.42	0.2950	0.0185	6.26
0°/45°	0.1	-1.0	0.2072	0.0095	4.57	0.1687	0.0082	4.8858
	1.0	0.0	0.2034	0.0009	0.43	0.1593	0.0074	4.6386
	10.0	1.0	0.2267	0.0245	10.79	0.1640	0.0042	2.5559
	50.0	1.7	0.2383	0.0146	6.12	0.1925	0.0025	1.2873

Table 3. Yarn/yarn frictional characteristics function of normal pressure at 1 mm/s

Orientation	Normal pressure (kPa)	$\mu_s$	Standard deviation [ $\sigma$ ]	$[\sigma/\mu_s]*100$ (%)	$\mu_k$	Standard deviation [ $\sigma$ ]	$[\sigma/\mu_k]*100$ (%)
0°/0°	3	0.4037	0.1766	43.74	0.3188	0.0126	3.96
	5	0.3478	0.0751	21.59	0.2831	0.0084	2.96
	10	0.2670	0.0058	2.16	0.2584	0.0068	2.64
	20	0.3336	0.0442	13.26	0.2822	0.0090	3.18
	50	0.3332	0.0122	3.67	0.3055	0.0059	1.93
0°/90°	3	0.2165	0.0164	7.57	0.1867	0.0091	4.88
	5	0.2186	0.0059	2.71	0.1913	0.0051	2.65

10	0.1832	0.0088	4.79	0.1644	0.0088	5.35
20	0.1984	0.0089	4.49	0.1748	0.0013	0.74
50	0.1911	0.0078	4.11	0.1656	0.0065	3.91

Table 4. Experimental friction coefficients of yarn/yarn at 35 kPa according to velocity

Orientation	Velocity (mm/s)	Log [velocity]	$\mu_s$	Standard deviation [ $\sigma$ ]	$[\sigma/\mu_s]*100$ (%)	$\mu_k$	Standard deviation [ $\sigma$ ]	$[\sigma/\mu_k]*100$ (%)
0°/0°	0.10	-1.0	0.3471	0.0017	0.49	0.2963	0.0412	13.89
	1.00	0.0	0.3406	0.0500	14.67	0.2914	0.0224	7.69
	10.00	1.0	0.3448	0.0320	9.28	0.2947	0.0104	3.53
	50.00	1.7	0.3664	0.0564	15.39	0.2997	0.0063	2.10
0°/90°	0.1	-1.0	0.1757	0.0002	0.13	0.1563	0.0068	4.37
	1.0	0.0	0.1825	0.0068	3.71	0.1739	0.0048	2.76
	10.0	1.0	0.2163	0.0075	3.45	0.1829	0.0026	1.43
	50.0	1.7	0.2458	0.0143	5.82	0.2243	0.0214	9.52